INTERNATIONAL JOURNAL OF NUMERICAL MODELLING: ELECTRONIC NETWORKS, DEVICES AND FIELDS
Int. J. Numer. Model. 2011; **24**:194–206
Published online 15 June 2010 in Wiley Online Library (wileyonlinelibrary.com). DOI: 10.1002/jnm.770

A conformal mapping-based approach for fast two-dimensional FEM electrostatic analysis of MEMS devices

Prasad S. Sumant[1,*,†], Andreas C. Cangellaris[2] and Narayana R. Aluru[1]

[1]*Department of Mechanical Science and Engineering, University of Illinois, 1206 W. Green St., Urbana, IL 61801, U.S.A.*
[2]*Department of Electrical and Computer Engineering, University of Illinois, 1406 W. Green St., Urbana, IL 61801, U.S.A.*

SUMMARY

In this paper, a methodology is proposed for expediting the coupled electro-mechanical two-dimensional finite element modeling of electrostatically actuated MEMS. The proposed methodology eliminates the need for repeated finite element meshing and subsequent electrostatic modeling of the device during mechanical deformation. We achieve this by mapping the deformed electrostatic domain to the reference undeformed domain 'conformally'. A 'conformal' map preserves the form of the Laplace equation and the boundary conditions; thus the electrostatic problem is solved only once in the undeformed electrostatic domain. The conformal map itself is generated through the solution of the same Laplace equation on the undeformed geometry and with displacement boundary conditions dictated by the movement of the mechanical domain. The proposed methodology is demonstrated through its application to the modeling of three MEMS devices with varying length-to-gap ratios, multiple dielectrics and complicated geometries. The accuracy of the proposed methodology is confirmed through comparisons of its results with results obtained using the conventional finite element solution. Copyright © 2010 John Wiley & Sons, Ltd.

Received 3 December 2008; Revised 11 January 2010; Accepted 16 April 2010

KEY WORDS: MEMS; FEM; electrostatically actuated; conformal mapping

1. INTRODUCTION

Micro-Electro-Mechanical (MEM) devices like switches, varactors and oscillators have shown great potential for the use in communication devices, sensors and actuators [1, 2]. They generally consist of thin, movable electrodes suspended over a fixed electrode. Electrode movement/deformation is exploited for different functions such as actuation, sensing and switching. These devices are designed to have thin beams and high length-to-gap ratios. Multiple dielectrics are included to enhance the performance.

The widespread insertion of MEMS devices in integrated electronics is critically dependent on the availability of accurate and computationally efficient, multi-physics CAD tools in support of device design iteration, optimization and performance degradation assessment. The focus of this paper is on electrostatically actuated MEMS, which are also the most widespread MEMS devices.

A detailed characterization of an electrostatically actuated MEMS device requires the solution of a coupled electro-mechanical problem. Several one-dimensional models and

*Correspondence to: Prasad S. Sumant, Department of Mechanical Science and Engineering, University of Illinois, 1206 W. Green St., Urbana, IL 61801, U.S.A.
†E-mail: psumant2@illinois.edu

Contract/grant sponsor: Defense Advanced Research Projects Agency (DARPA)

approximate analytical expressions have been presented for calculating the electro-mechanical response of the switch [3]. There have also been some efforts toward the development of one-dimensional models for reliability analysis [4]. Such models are good for quick design evaluation and understanding of the device operation. However, these methods are limited in their description of the governing physics and lack the modeling detail and simulation accuracy needed for design optimization and performance degradation assessment. To provide for the needed modeling rigor and solution accuracy, finite element methods (FEM), boundary elements methods (BEM) and hybrid FEM-BEM schemes are used. For example, MEMCAD [5] uses ABAQUS, a commercial FEM package for the mechanical analysis and a BEM-based program FASTCAP [6] for the electrostatic analysis. In the absence of material inhomogeneity, BEM is the method of choice for the electrostatic problem, since only the surface of the conducting electrodes need be discretized. However, for devices with significant dielectric material inhomogeneity and, in general, substantial geometric complexity, an FEM solution to the electrostatic problem offers modeling versatility and formulation simplicity. To avoid the numerical error introduced by the truncation of the finite element grid for the case of unbounded geometries, hybrid formulations where an FEM model of the interior is complemented by a BEM statement on the surface used for truncating the computational domain is possible [7, 8].

There are some inherent computational challenges for performing a coupled electro-mechanical solution. To provide a framework for their discussion, let us consider the application of a two-dimensional FEM model for a coupled electro-mechanical analysis of an electrostatically actuated MEMS device. In order to keep the presentation simple, it is assumed that a relaxation-based algorithm rather than a Newton method [9] is used for the coupling of the electrostatic and the mechanical domains. Our proposed approach does not rely on this assumption. The relaxation-based algorithm is as follows:

Algorithm 1

Perform an electrostatic analysis in the non-deformed geometry to calculate forces for use in the mechanical domain.

Repeat the following **until** an equilibrium state is reached:

1. Do mechanical analysis (in the non-deformed geometry) to compute structural displacements.
2. Update the geometry of the movable electrode using computed displacements.
3. Compute the electric field by electrostatic analysis (deformed geometry).
4. Compute electrostatic forces on the movable membrane in the deformed configuration.
5. Transform the electrostatic forces to the original non-deformed configuration.

During each step of the relaxation-based algorithm the beam deforms modifying the electrostatic BVP domain. In the context of BEM, a Lagrangian formulation was proposed in [10] to eliminate the need for such geometry update. In the context of FEM, the geometry update necessitates a change in the mesh used for the finite element solution of the electrostatic BVP. This is depicted for the case of the cantilever beam electrode suspended over a fixed bottom electrode in Figure 1. One approach for updating the mesh is to treat it as another elastic solid with some appropriate elastic properties, and use the deflection of the movable beam as input boundary displacements [11, 12]. Then, using a finite element solution to the elasticity problem, the new mesh is obtained as a displacement of the previous one. This process is also known as mesh updating or mesh morphing. Similar smoothing techniques are commonly found in commercial FEM software packages such as ANSYS [13]. An alternative approach is to simply re-mesh the deformed structure at each relaxation step. Both approaches require a re-factorization of the electrostatic stiffness matrix and hence increase considerably the computational cost of the relaxation algorithm. There have been many efforts in the context of finite difference time domain modeling of curved boundaries [14–16]. In particular, in [16] a solution of the complex Laplace equation was used to generate a 2D locally conformal grid

DOI: 10.1002/jnm

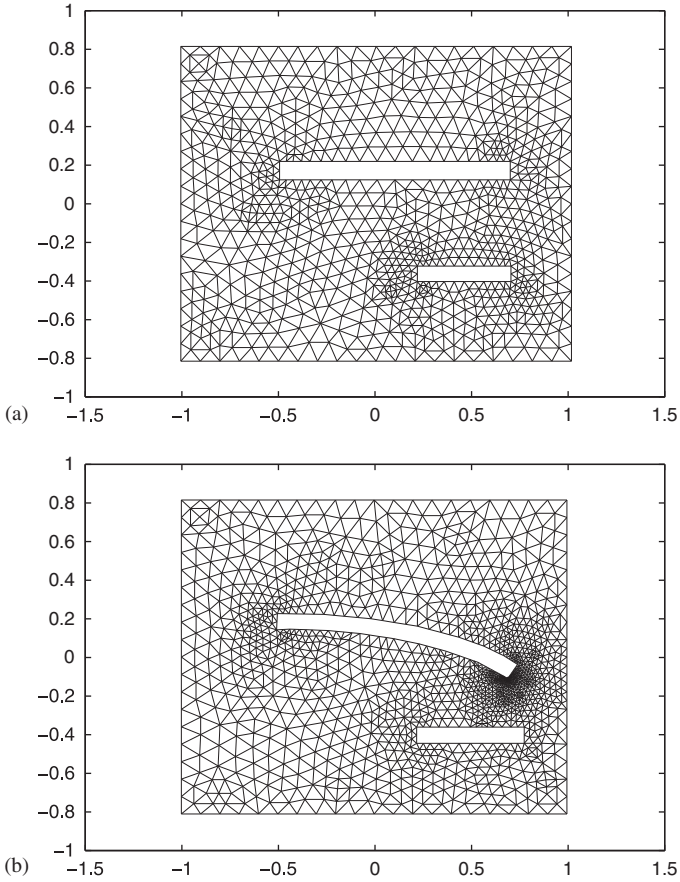

Figure 1. Conventional FEM electro-mechanical modeling: (a) electrostatic BVP meshing of non-deformed configuration and (b) electrostatic BVP meshing of deformed configuration.

between curved boundaries and a remaining rectangular grid. The only geometry considered however was that of a uniform cylinder.

The methodology proposed in this paper is aimed at overcoming the aforementioned shortcomings of the two-dimensional FEM solution of the electrostatic BVP by eliminating the need for mesh update. The paper is organized as follows. In Section 2, the proposed methodology for the solution of the electrostatic BVP without mesh updating is presented. This is followed by its demonstration in Section 3 to the modeling of three electrostatically actuated MEMS devices. These numerical studies provide for the verification of the proposed methodology and the assessment of its accuracy.

2. PROPOSED METHODOLOGY

2.1. Mathematical formulation

Let us consider the most generic representation of a MEMS device in terms of a movable top electrode, a bottom electrode and region consisting of different dielectrics in between the two electrodes as shown in Figure 2. Typically, MEMS devices have the top electrode moving through a region of a homogeneous dielectric (which is most commonly air) represented by ε_h in the figure. Also, a MEMS device can consist of regions of different layers of dieletric as represented by $\varepsilon(\vec{r})$ in the figure. Note, however that the formulation does not rely on this assumption.

Let us consider an intermediate deformed configuration of the top electrode as shown in Figure 2a. The coupling between the mechanical and electrical domains happens through the

DOI: 10.1002/jnm

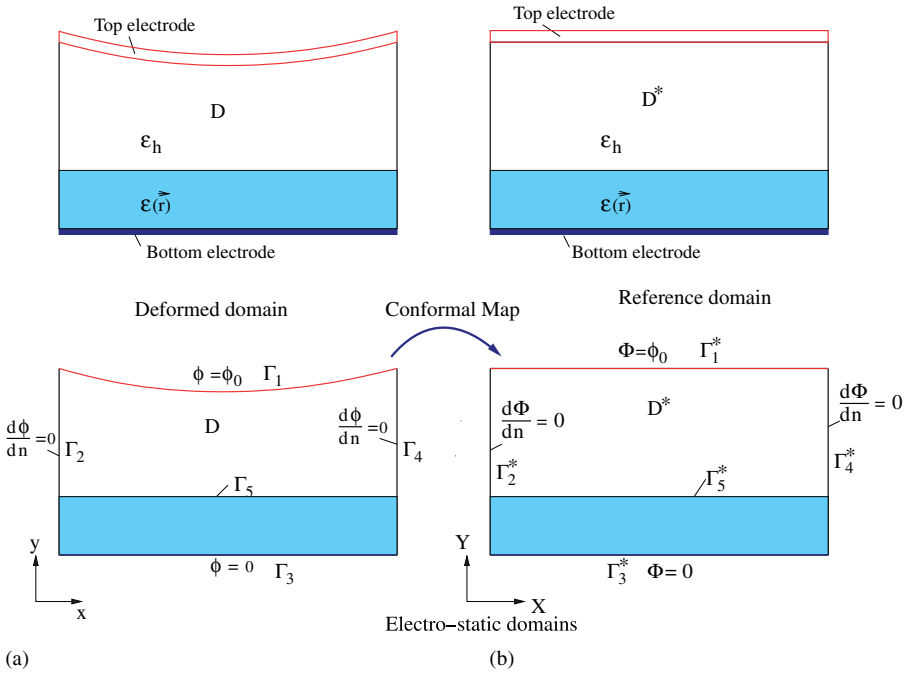

Figure 2. Conformal mapping from deformed domain to reference domain.

electrostatic pressure, P, on the movable electrode. It is given by,

$$P = \frac{\rho_s^2}{2\varepsilon} \tag{1}$$

where the electric charge density on the conductor surface (Γ_s) is given by

$$\rho_s = \hat{n} \cdot (-\varepsilon \nabla \phi) \tag{2}$$

In the above equation $\hat{n}$ is the outward pointing unit normal on the conductor surface and ϕ represents the electric potential. The computation of charge density requires the solution of a Laplace equation in the deformed domain D with the typical boundary conditions as shown in Figure 2a. Mathematically,

$$\nabla_x \cdot (\varepsilon(x, y) \nabla_x \phi(x, y)) = 0 \quad \text{in } D \tag{3}$$

$$\phi = \phi_0 \quad \text{on } \Gamma_1 \tag{4}$$

$$\phi = 0 \quad \text{on } \Gamma_3 \tag{5}$$

$$\frac{\partial \phi}{\partial n} = 0 \quad \text{on } \Gamma_2, \Gamma_4 \tag{6}$$

The objective of our proposed method is to transform this problem in the domain D to one in the domain D^*, which corresponds to the initial undeformed state. Note that when performing this transformation we want to preserve the solid dielectrics. So the mapping essentially is a mapping of the homogeneous (air) medium next to the movable electrode. Thus, we can consider the governing Laplace equation in a piecewise fashion, and work with,

$$\nabla_x \cdot (\varepsilon_h \nabla_x \phi(x, y)) = 0 \tag{7}$$

$$\nabla_x^2 \phi(x, y) = 0 \tag{8}$$

Let $w = f(z) = X + iY$ be an analytic function that maps a domain D (with (x,y) coordinates) one–one and conformally to the domain D^* (with (X,Y) coordinates) and let the mapping be

DOI: 10.1002/jnm

expressed as.

$$\begin{aligned} x &= X+u \\ y &= Y+v \end{aligned} \tag{9}$$

Let $\Phi(X,Y)$ correspond one–one to $\phi(x,y)$. Using this transformation we have,

$$\frac{\partial \phi}{\partial x} = \frac{\partial \Phi}{\partial X}\frac{\partial X}{\partial x} + \frac{\partial \Phi}{\partial Y}\frac{\partial Y}{\partial x} \tag{10}$$

$$\frac{\partial \phi}{\partial y} = \frac{\partial \Phi}{\partial X}\frac{\partial X}{\partial y} + \frac{\partial \Phi}{\partial Y}\frac{\partial Y}{\partial y} \tag{11}$$

The governing equation (8) can be transformed as,

$$\begin{aligned} \nabla_x^2 \phi(x,y) = {} & \frac{\partial^2 \Phi}{\partial X^2}\left[\left(\frac{\partial X}{\partial x}\right)^2 + \left(\frac{\partial X}{\partial y}\right)^2\right] + \frac{\partial^2 \Phi}{\partial Y^2}\left[\left(\frac{\partial Y}{\partial x}\right)^2 + \left(\frac{\partial Y}{\partial y}\right)^2\right] \\ & + \left(\frac{\partial^2 \Phi}{\partial X \partial Y}\frac{\partial^2 \Phi}{\partial Y \partial X}\right)\left(\frac{\partial X}{\partial x}\frac{\partial Y}{\partial x} + \frac{\partial X}{\partial y}\frac{\partial Y}{\partial y}\right) + \frac{\partial \Phi}{\partial u}\nabla^2 X + \frac{\partial \Phi}{\partial y}\nabla^2 Y \end{aligned} \tag{12}$$

The last three terms in the above equation go to zero because $z = f(X,Y)$ is analytic [17]. More specifically, using Cauchy–Reimann equations [17],

$$\frac{\partial X}{\partial x} = \frac{\partial Y}{\partial y} \tag{13}$$

$$\frac{\partial X}{\partial y} = -\frac{\partial Y}{\partial x} \tag{14}$$

Thus, we get

$$\nabla_x^2 \phi(x,y) = \frac{\partial^2 \Phi}{\partial X^2}\left[\left(\frac{\partial X}{\partial x}\right)^2 + \left(\frac{\partial X}{\partial y}\right)^2\right] + \frac{\partial^2 \Phi}{\partial Y^2}\left[\left(\frac{\partial Y}{\partial x}\right)^2 + \left(\frac{\partial Y}{\partial y}\right)^2\right] = 0 \tag{15}$$

$$\nabla_X^2 \Phi(X,Y) = 0 \tag{16}$$

So the Laplace equation remains invariant under a conformal mapping. Also, it can be shown that Dirichlet conditions map to Dirichlet conditions on the corresponding boundary and so also the Neumann boundary conditions [17]. Thus the original Laplace problem in the domain D is transformed to a domain D^*

$$\nabla_X.(\varepsilon \nabla_X \Phi(X,Y)) = 0 \quad \text{in } D^* \tag{17}$$

$$\Phi = \phi_0 \quad \text{on } \Gamma_1^* \tag{18}$$

$$\Phi = 0 \quad \text{on } \Gamma_3^* \tag{19}$$

$$\frac{\partial \Phi}{\partial n} = 0 \quad \text{on } \Gamma_2^*, \Gamma_4^* \tag{20}$$

This means that all the intermediate deformed states D can be transformed to the same initial state D^*, thus eliminating the need for doing a mesh update and matrix refactorization. So if we can develop a map $z = f(X,Y)$ such that f is analytic we can achieve the above transformation of the Laplace equation from domain D to D^*. Now, for f to be analytic,

$$\frac{\partial X}{\partial x} = \frac{\partial Y}{\partial y} \tag{21}$$

$$\frac{\partial X}{\partial y} = -\frac{\partial Y}{\partial x} \tag{22}$$

DOI: 10.1002/jnm

Alternatively, this can be written as,

$$\frac{\partial x}{\partial X} = \frac{\partial y}{\partial Y} \tag{23}$$

$$\frac{\partial y}{\partial X} = -\frac{\partial x}{\partial Y} \tag{24}$$

Using the above with Equation (9) leads to:

$$\frac{\partial u}{\partial X} = \frac{\partial v}{\partial Y} \tag{25}$$

$$\frac{\partial v}{\partial X} = -\frac{\partial u}{\partial Y} \tag{26}$$

Above equations can be converted into one variable v, and that is

$$\frac{\partial^2 v}{\partial X^2} + \frac{\partial^2 v}{\partial Y^2} = 0 \tag{27}$$

The boundary conditions for this problem are obtained from the mechanical displacements of the top electrode. To calculate the electrostatic pressure on the top electrode in the deformed domain, we use,

$$P(x, y) = \tfrac{1}{2}\varepsilon|\nabla_x \phi(x, y)|^2 \tag{28}$$

where $\bigtriangledown_x \phi(x,y)$ is obtained using

$$\nabla_x \phi(x, y) = F^{-\mathrm{T}} \nabla_X \Phi(X, Y) \tag{29}$$

where F is given by,

$$F = \begin{bmatrix} 1+\frac{\partial u}{\partial X} & \frac{\partial v}{\partial X} \\ \frac{\partial u}{\partial Y} & 1+\frac{\partial v}{\partial Y} \end{bmatrix} \tag{30}$$

Now $\bigtriangledown_X \phi(X, Y)$ is constant at every relaxation step and needs to be computed only once. The thing that is updated at every step is F, which is obtained from a solution of the following equation:

$$\nabla_X.(\varepsilon \nabla_X v(X, Y)) = 0 \quad \text{in } D^* \tag{31}$$

$$v = v_{\text{top electrode}} \quad \text{on } \Gamma_1^* \tag{32}$$

$$v = 0 \quad \text{on } \Gamma_2^*, \Gamma_3^*, \Gamma_4^*, \Gamma_5^* \tag{33}$$

Note that the ∇_X^2 operator is the same as the one for electrostatic problem in the undeformed domain (Equation (17)) and needs to be computed only once.

The algorithm for performing the FEM-based electro-mechanical analysis utilizing the aforementioned approach is as follows:

Algorithm 2

1. Solve the electrostatic FEM problem in the undeformed domain (Equation 17).
2. Calculate the matrix F (Equation (30)) and use the electric field in the deformed domain using Equation (29).
3. Loads/boundary conditions for the mechanical solution are computed using the calculated values of the electric field and its direction along the movable electrode.
4. Solve the mechanical FEM to compute the deflection/deformation of the movable electrode.
5. Use the calculated displacement $v(x,y)$ of the movable electrode, update the boundary condition along Γ_1. The electrical mesh remains the same, only the dirichlet boundary conditions are modified.
6. Solve Equation (33).
7. Go to step 2 and repeat until convergence

DOI: 10.1002/jnm

Clearly, since the geometry does not change, there is no need for re-meshing and re-generating the FEM matrix for the electrostatic BVP. Thus, in subsequent steps, the same factorization of the electrostatic FEM matrix can be used. This results in computation savings at every relaxation step.

2.2. Computational complexity analysis

In the following we compare the computational complexity of the two algorithms, Algorithm 1 of Section I used in the standard FEM electro-mechanical analysis, and Algorithm 2, resulting from the implementation of the methodology proposed in this paper for the FEM solution of the electrostatic BVP. For this purpose, the following notation will be used:

- N_{m}: number of nodes in the FEM mesh for the mechanical problem
- N_{e}: number of nodes in the FEM mesh for the electrostatic problem
- N_i: number of nodes at the boundary of the movable electrode for the mechanical problem and on S_f for the auxiliary electrostatic problem
- N_{iter}: number of relaxation steps for convergence

Table I summarizes the comparison of the two algorithms. An explanation of the entries in Table I is as follows. For both the algorithms, the stiffness matrix for the mechanical domain needs to be assembled and factored only once. The FEM system for the mechanical domain needs to be solved at every relaxation step for both algorithms. For Algorithm 1, the stiffness matrix for the electrostatic problem needs to be reassembled and factored at every relaxation step as the geometry of the electrostatic problem changes at every step due to electrode deformation. In contrast, in Algorithm 2, this has to be done only once, since the deformed geometry is mapped conformally onto the un-deformed geometry and that preserves the Laplace equation. Furthermore, in Algorithm 1, an FEM mesh update is required at every relaxation step. This cost is completely eliminated in Algorithm 2.

Assuming $N_{\mathrm{iter}} = 10$, the computational cost for each algorithm is obtained from the entries of Table I, as follows:

$$\text{Algorithm 1: } O(N_{\mathrm{m}}^{1.5}+13N_{\mathrm{e}}^{1.5}+11N_{\mathrm{m}}+42N_{\mathrm{e}}+20N_i) \approx O(N_{\mathrm{m}}^{1.5}+13N_{\mathrm{e}}^{1.5}+40N_{\mathrm{e}}) \tag{34}$$

$$\text{Algorithm 2: } O(N_{\mathrm{m}}^{1.5}+N_{\mathrm{e}}^{1.5}+11N_{\mathrm{m}}+2N_{\mathrm{e}}+20N_i) \approx O(N_{\mathrm{m}}^{1.5}+N_{\mathrm{e}}^{1.5}) \tag{35}$$

Thus Algorithm 2, based on the proposed methodology, is roughly 10 times more efficient than Algorithm 1.

Table I. Conformal Mapping from deformed domain to reference domain.

Step	Order	Algorithm 1	Algorithm 2
Assembly			
Stiffness matrix for mechanical domain	N_{m}	1	1
Stiffness matrix for electrical domain	N_{e}	N_{iter}	1
Stiffness matrix for pseudo-elastic (electrical) domain	$2N_{\mathrm{e}}$	1	0
Factorization of stiffness matrix			
Stiffness matrix for mechanical domain	$N_{\mathrm{m}}^{1.5}$	1	1
Stiffness matrix for electrical domain	$N_{\mathrm{e}}^{1.5}$	N_{iter}	1
Stiffness matrix for pseudo-elastic (electrical) domain	$(2N_{\mathrm{e}})^{1.5}$	1	0
Forward and backward solve for linear system			
For mechanical domain	N_{m}	N_{iter}	N_{iter}
For electrical domain	N_{e}	N_{iter}	1
For pseudo-elastic (electrical) domain	$(2N_{\mathrm{e}})$	N_{iter}	0
Update interface conditions			
To calculate electrostatic forces for mechanical domain	N_i	N_{iter}	N_{iter}
To calculate mechanical displacements for electrical domain	N_i	0	N_{iter}
To calculate mechanical displacements for pseudo-elastic domain	N_i	N_{iter}	0

DOI: 10.1002/jnm

3. NUMERICAL STUDIES

Three case studies are presented next for assessing the performance and demonstrating the accuracy and versatility of the proposed method. These studies involve some of the most common electrode geometries used in electrostatically actuated MEMS devices. Each individual case study presents some unique challenges that, as it will be demonstrated, are successfully handled by the proposed method.

3.1. Cantilever series switch

One of the most important RF MEMS switches is the cantilever series switch [3] depicted in Figure 3(a). It consists of a beam suspended over a bottom ground electrode, which is part of a microwave, planar transmission line. The bottom ground electrode is on top of a silicon substrate. The purpose of this case study is to demonstrate the applicability and accuracy of the proposed method for handling cantilever geometries with asymmetric placement of electrodes.

The modeled geometry is depicted in Figure 3(b). Note that the silicon substrate is not included in this study. The top electrode is 150 μm in length, 2 μm in thickness. Young's modulus E is 170 GPa and Poisson's ratio v is 0.34. The bottom electrode is 50 μm in length, 2 μm in thickness, and located 100 μm from the leftmost end of the top electrode. The gap length is 4.5 μm.

A FEM solver based on Lagrangian mapping [10] is used for the implementation of Algorithm 1 and for providing the reference solution. The applied voltage is varied up to its pull in value and the tip deflections obtained using the two methods are compared in Figure 4. The proposed methodology is seen to be very accurate.

3.2. Simply supported RF MEMS capacitive switch

The MEMS device under study in this section is the simply supported RF capacitive switch of [18], depicted in Figure 5. It consists of an Au beam for the top movable electrode, suspended over a center ground conductor, which is part of a coplanar waveguide. The center ground electrode is placed on top of a SiO_2 layer, which is on top of a silicon substrate. A thin layer of

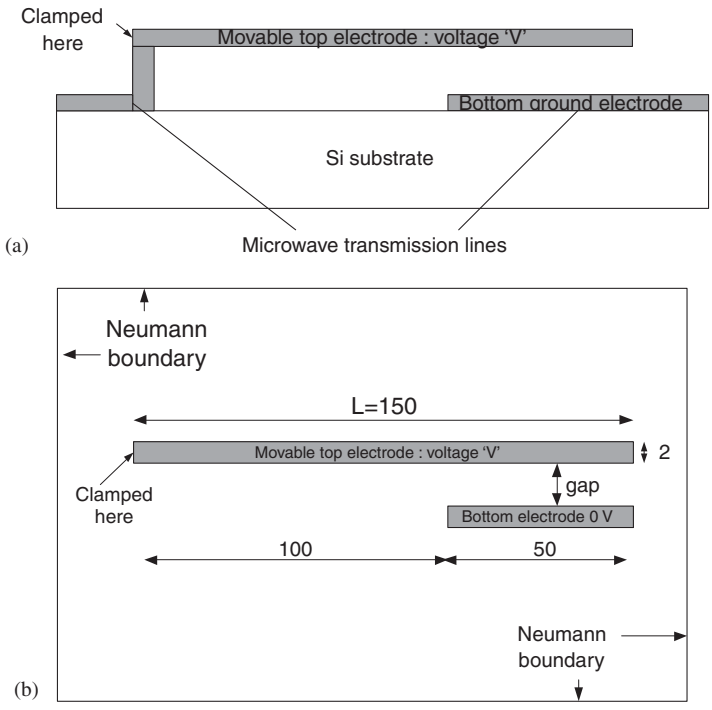

Figure 3. Cantilever series switch: (a) actual device and (b) modeled geometry. All dimensions in microns.

DOI: 10.1002/jnm

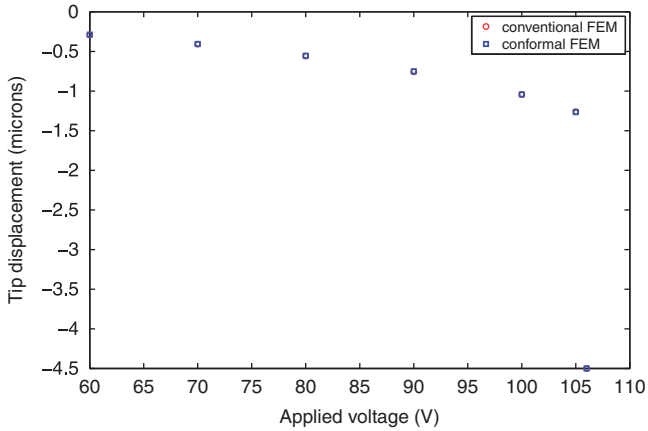

Figure 4. Tip deflection of cantilever.

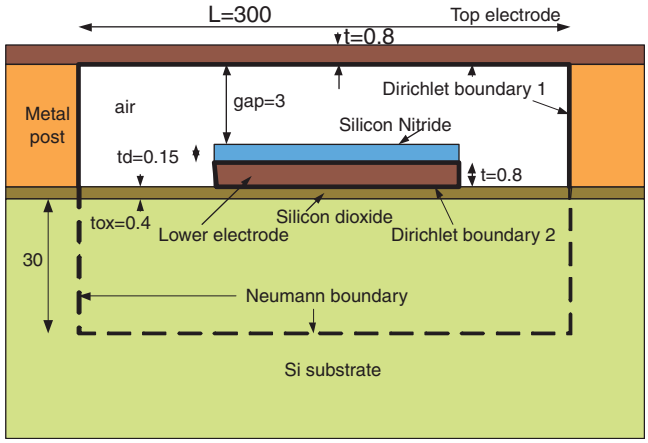

Figure 5. RF MEMS switch. All dimensions in microns.

silicon nitride is deposited on top of the center conductor. This layer of dielectric prevents direct metal-to-metal contact of the two electrodes. The presence of the metal posts at which the top beam is attached provide for a natural truncation of the computational domain on the two sides and the top. A truncation boundary is introduced in the Si substrate, resulting in the cross-sectional geometry of the computational domain depicted in Figure 5.

Since the width of the top electrode is much larger than the vertical thickness, a two-dimensional analysis, involving the cross-sectional geometry depicted in Figure 5 suffices. The geometric dimensions that define the cross-sectional geometry are as follows. The length of the top electrode is 300 μm. Its thickness, t, is 0.8 μm. The length of the lower electrode is 100 μm and its thickness, t_e, is 0.8 μm. The silicon oxide layer thickness, t_{ox}, is 0.4 μm. The silicon nitride thickness, t_d, is 0.15 μm. The relative permittivities of the Si_3N_4 and SiO_2 layers are, respectively, 7.6 and 3.9. The relative permittivity of Si is taken to be 11.0. For the Au beam, Young's modulus, E, is 80 GPa and Poisson's ratio v is 0.42. The thickness of the Si layer is 30 μm. The boundary condition imposed at the bottom truncation boundary for the electrostatic BVP is one of zero electric flux density.

Like in the previous case, we use a FEM solver based on the Lagrangian formulation for generating the reference solution, based on the application of Algorithm 1. Figure 6 depicts the computed center deflections of the top electrode for different values of voltages upto pull in. The proposed methodology is seen to be very accurate up to pull in.

DOI: 10.1002/jnm

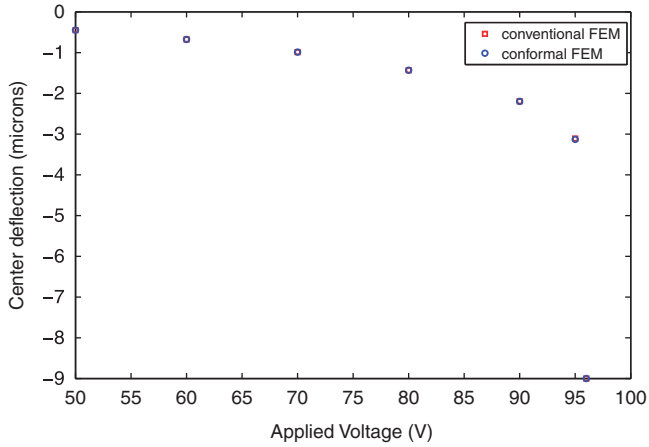

Figure 6. Center deflection of RF MEMS capacitive switch.

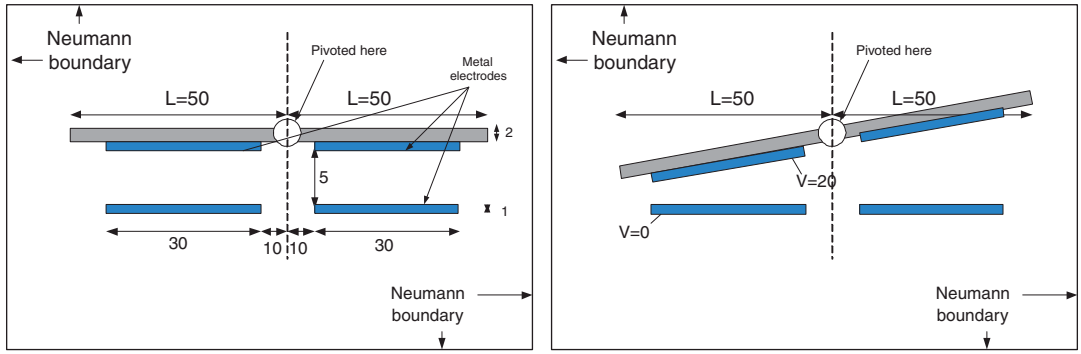

Figure 7. Torsion micro mirror: (a) undeformed state and (b) deformed state. All dimensions in microns.

3.3. Torsional micro-mirror

Torsional micro-mirrors have been widely used in applications such as spatial light modulators, optical crossbar switches, adaptive optics and digital projection displays [19, 20]. This case study focuses on the application of the proposed method to the electrostatic analysis of a typical torsion micro-mirror device. Since the device involves rotation of electrodes and thus substantial fringing, it serves as an ideal candidate for assessing the limits of validity of the proposed methodology.

Figure 7a depicts a generic version of the most general design of a torsion micro-mirror reported in the literature [19, 21]. It consists of two metal electrodes mounted on a beam that is pivoted at the center. The beam is free to rotate about the pivot. There are two bottom electrodes located at a certain distance below the top electrodes. A voltage applied between two electrodes on one side produces an electrostatic force of attraction between them, which results in a torque on the beam. This torque causes the beam to rotate and rest at an angle to the original position. The most important design parameter of a torsion micro-mirror is the maximum angle of rotation before it snaps and pulls in. This parameter depends on the gap between the top and bottom electrodes and the length of the top beam.

In micro-mirror devices reported in the literature, most length-to-gap ratios are found to be greater than 50:1. However, in order to assess the limits of validity of the proposed method, we consider a design of a micro-mirror with a length-to-gap ratio of 10:1. We consider the state of a torsion mirror just before/at pull in. In other words, we consider the maximum rotation of the

DOI: 10.1002/jnm

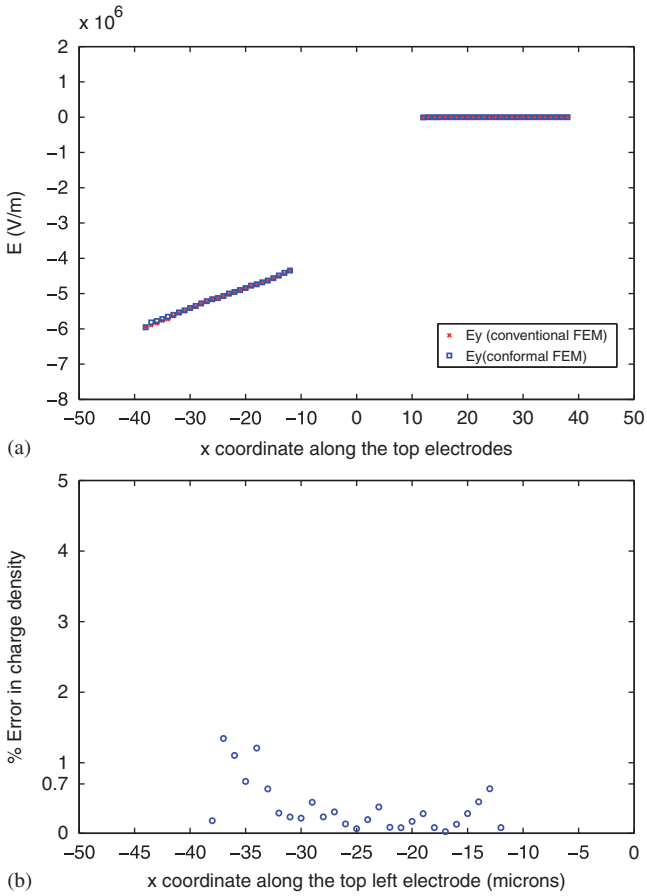

Figure 8. Torsion micro mirror electrostatic analysis: (a) electric field comparison with conventional FEM and (b) percentage error in charge density along the top left electrode.

top beam. From [21], the angle α at which the beam pulls in is given by

$$\alpha = 0.44\frac{d}{L} \tag{36}$$

where d is the distance between the top and bottom electrodes and L is the length of the beam on one side of the pivot.

We apply the proposed method (to the undeformed configuration Figure 7a) to calculate the electric field along the top electrodes and compare the results with those obtained using the conventional FEM analysis for the beam in the deformed configuration (Figure 7b). The comparison is shown in Figure 8a. It is clear that a very good agreement is observed. The electric charge density is also computed. The % error in the calculated charge density along the top left electrode is plotted in Figure 8b. The maximum error is about 1.2%, which occurs at the extreme left. Along the beam the error is less than 0.7% demonstrating the accuracy of our proposed method.

4. CONCLUSIONS

In summary, we have proposed a methodology for expediting the coupled electro-mechanical two-dimensional finite element modeling of electrostatically actuated MEMS devices. The enhanced efficiency of the proposed methodology is achieved by eliminating the mesh updating, stiffness matrix calculation and stiffness matrix factorization, associated with the FEM solution of the electrostatic problem at each step of a relaxation-based algorithm, which is assumed to be

DOI: 10.1002/jnm

used for the electro-mechanical simulation. The way this is accomplished is through the definition of a conformal map from the deformed to the undeformed geometry. The 'conformal map' is obtained through the solution of the same Laplace equation on the undeformed geometry. The boundary conditions are obtained from the displacement of the movable electrode.

The proposed methodology was verified through its application to the modeling of three classes of MEMS geometries, namely, a cantilever series switch, a simply supported RF MEMS capacitive switch and a torsion micro mirror. The dimensions and material properties used for the verification studies were the representative of practical MEMS devices. Through comparisons with reference solutions it was shown that the proposed methodology is very accurate for the three classes of the electrostatically actuated MEMS devices considered. This was achieved at an estimated one order-of-magnitude reduction in the computational cost compared with a standard FEM-based electro-mechanical modeling.

ACKNOWLEDGEMENTS

This research was supported in part by the Defense Advanced Research Projects Agency (DARPA), under the N/MEMS Science & Technology Fundamentals Research Program.

REFERENCES

1. Yao J. RF MEMS from a device perspective. *Journal of Micromechanics and Microengineering* 2000; **10**:9–38.
2. Tillmans H, Raedt W, Beyne E. MEMS for wireless communications: 'from RF-MEMS components to RF-MEMS-SIP'. *Journal of Micromechanics and Microengineering* 2003; **13**:139–163.
3. Varadan V, Vinoy K, Jose K. *RF MEMS and Their Applications*. John Wiley: New York, 2003.
4. van Spengen W, Peurs R, Mertens R, Wolf I. A comprehensive model to predict the charging and reliability of capacitive RF MEMS switches. *Journal of Micromechanics and Microengineering* 2004; **14**:514–521.
5. Senturia S, Harris R, Johnson B, Songmin K, Nabors K, Shulman M, White J. A computer-aided design system for microelectromechanical systems (MEMCAD). *Journal of Microelectromechanical systems* 1992; **1**:3–13.
6. Nabors K, White J. FastCap: a multi-pole accelerated 3-D capacitance extraction program. *IEEE Transactions on Computer-Aided Design* 1991; **10**:1447–1459.
7. Jin J. The Finite Element Method in Electromagnetics. John Wiley: New York, 2002.
8. Li G, Aluru N. Hybrid techniques for electrostatic analysis of nanoelectromechanical systems. *Journal of Applied Physics* 2004; **96**:2221–2231.
9. De S, Aluru N. Full-Lagrangian schemes for dynamic analysis of electrostatic MEMS. *Journal of Microelectromechanical Systems* 2004; **13**:737–758.
10. Li G, Aluru N. A Lagrangian approach for electrostatic analysis of deformable conductors. *Journal of Microelectromechanical systems* 2002; **11**: 245–254.
11. Soma A, Bona F, Gugliotta A, Mola E. Meshing approach in non-linear FEM analysis of microstructures under electrostatic loads. *Proceedings of SPIE* 2001; **4408**:216–225.
12. Chiandussi G, Bugeda G, Onate E. A simple method for automatic update of finite element meshes. *Communications in Numerical Methods in Engineering* 2000; **16**:1–19.
13. Zhulin V, Owen S, Ostergaard D. Finite element based electrostatic-structural coupled analysis with automated mesh morphing. *International Conference on Modeling and Simulation of Microsystems*, San Diego, CA, 2000; 501–504.
14. Fusco M. FDTD algorithm in curvilinear coordinates. *IEEE Transactions on Antennas and Propagation* 1990; **38**(1):76–89.
15. Jurgens T, Taflove A, Umashankar K, Moore T. Finite-difference time-domain modeling of curved surfaces. *IEEE Transactions on Antennas and Propagation* 1992; **40**(4):357–366.
16. Pan G, Cheng D, Gilbert B. 2D FDTD modelling of objects with curved boundaries, using embedded boundary orthogonal grids. *IEE Proceedings on Microwaves, Antennas and Propagation* 2000; **147**(5):399–405.
17. Jeffrey A. Complex Analysis and Applications. Chapman & Hall: London, 2006.
18. Hamad E, Omar A. An improved two-dimensional coupled electrostatic-mechanical model for RF MEMS switches. *Journal of Micromechanics and Microengineering* 2006; **16**:1424–1429.
19. Zhang X, Chau F, Quan C, Lam Y, Liu A. A study of the static characteristics of a torsion micromirror. *Sensors and Actuators A* 2001; **90**:73–81.
20. Buhler J, Funk J, Korvink J, Steiner F, Sarro P, Baltes H. Electrostatic Aluminum micromirrors using double-pass metallization. *Journal of Microelectromechanical systems* 1997; **6**(2):126–135.
21. Degani O, Socher E, Lipson A, Leitner T, Setter D, Kaldor S, Nemirovsky Y. Pull-in study of an electrostatic torsion microactuator. *Journal of Microelectromechanical systems* 1998; **7**(4):373–379.

DOI: 10.1002/jnm

AUTHORS' BIOGRAPHIES

Prasad S. Sumant received his BTech (Bachelor of Technology) in Mechanical Engineering and MTech (Master of Technology) in Computer Aided Design and Automation (CADA) from the Indian Institute of Technology Bombay (IITB), India, in 2004. He joined the Department of Mechanical Science and Engineering at the University of Illinois at Urbana-Champaign (UIUC) in Fall 2005 and is currently working towards his PhD degree.

His research interests include computational methods for design and analysis of MEMS, computational electromagnetics and numerical techniques in engineering. He is a student member of IEEE. He is a recipient of the Outstanding Scholar Fellowship (2005-Present) from the Department of Mechanical Science and Engineering at UIUC. He was elected to the honor society of Phi Kappa Phi in 2007.

Andreas C. Cangellaris is the M. E. Van Valkenburg Professor in Electrical and Computer Engineering, at the University of Illinois, Urbana-Champaign. His expertise and research interests are in electromagnetism and its applications to the advancement of modeling methodologies and CAD tools in support of electrical performance analysis and noise-aware design of integrated electronic systems. He was the co-founder of the IEEE Topical Meeting on Electrical Performance of Electronic Packaging in 1991. He is a Fellow of IEEE and is currently serving as Editor of the IEEE Press Series on Electromagnetic Wave Theory, Associate Editor of the IEEE Transactions on Advanced Packaging, and as Distinguished Lecturer for the IEEE Microwave Theory & Techniques Society. In 2005 he received the Alexander von Humboldt Research Award from the Alexander von Humboldt Foundation, Germany, for outstanding contributions to electromagnetic theory. In 2000 he received the University of Illinois, ECE Department Outstanding Faculty Teaching Award.

Narayana R. Aluru is currently a Professor in the Department of Mechanical Science and Engineering at University of Illinois at Urbana-Champaign. He is also affiliated with the Beckman Institute for Advanced Science and Technology, the Department of Electrical and Computer Engineering and the Bioengineering Department at UIUC.

He received the BE degree with honors and distinction from the Birla Institute of Technology and Science (BITS), Pilani, India, in 1989, the MS degree from Rensselaer Polytechnic Institute, Troy, NY, in 1991, and the PhD degree from Stanford University, Stanford, CA, in 1995. He was a Postdoctoral Associate at the Massachusetts Institute of Technology (MIT), Cambridge, from 1995 to 1997. In 1998, he joined the University of Illinois at Urbana-Champaign (UIUC) as an Assistant Professor. He received the NSF CAREER award in 1999, the NCSA faculty fellowship in 1999 and 2006, the 2001 CMES Distinguished Young Author Award, the Xerox Award for Faculty Research in 2002, the ASME Gustus L. Larson Memorial Award in 2006, the USACM Gallagher Young Investigator Award in 2007 and was named a Willett Faculty Scholar by the College of Engineering at UIUC for the period 2002-2008. He is a Subject Editor of the IEEE/ASME Journal of Microelectromechanical Systems, served as the Associate Editor of IEEE Transactions in Circuits and Systems II for 2004-2005, and currently serves on the Editorial Board of a number of other journals.

DOI: 10.1002/jnm